

# A Robotic Hyperspectral Scanning Framework for Endoscopy

F.B. Avila-Rencoret<sup>1,2</sup>, D.S. Elson<sup>1,2</sup>, G. Mylonas<sup>2</sup>

<sup>1</sup>The Hamlyn Centre for Robotic Surgery, <sup>2</sup>Department of Surgery and Cancer

Imperial College London, UK.

fba13@ic.ac.uk

## INTRODUCTION

Gastrointestinal (GI) endoscopy is the gold-standard procedure for detection and treatment of dysplastic lesions and early stage GI cancers [1]. In spite of its proven effectiveness, its sensitivity remains suboptimal due to the subjective nature of the examination, which is substantially reliant on human-operator skills. For bowel cancer, colonoscopy can miss up to 22% of dysplastic lesions, with even higher miss rates for small (<5 mm diameter) and flat lesions [2]. The proposed system seeks to improve the sensitivity of GI endoscopy by automated scanning and real-time classification of wide tissue areas based on their hyperspectral (HS) features. A “hot-spot” map is generated to highlight dysplastic or cancerous lesions for further scrutiny or concurrent resection [3]. The device works as an add-on accessory to any conventional endoscope and to our knowledge is the first of its kind.

## ENGINEERING SPECIFICATIONS

The device comprises a radial array of optical sensors that can be partially rotated and translated along the GI tract

while acquiring optical data (Fig. 1, A-C). The optical sensor array consists of eight single-point diffuse reflectance spectroscopy (DRS) fibre optic probes, introduced in a collapsed configuration as an over-tube add-on accessory to any conventional endoscope. Deployment of the collapsed sensors is achieved by externally actuated tendons and respective Bowden force transmission conduits. Each probe contains an illumination fibre that emits white light (Fig. 1, A). The light is diffusely scattered inside the tissue and a parallel fibre collects and transmits it to a spectrograph (V10, SPECIM) where is diffracted into its spectrum and finally captured by an sCMOS camera (optiMOS, QImaging). From each spectral image acquired, an image processing sub-routine converts it to 8 DRS spectra (Fig. 1, A-left). The device is simultaneous and continuously translated and rotated to scan and obtain a 2D map of the entire lumen under interrogation. Rotation is provided by an external hollow rotary actuator through which the endoscope is inserted (SMH88, Stogra). Translation along the lumen using the endoscope as a rail is achieved by a stepper motor (SM56, Stogra) actuating a linear stage (404XE, Parker). Actuation control, data

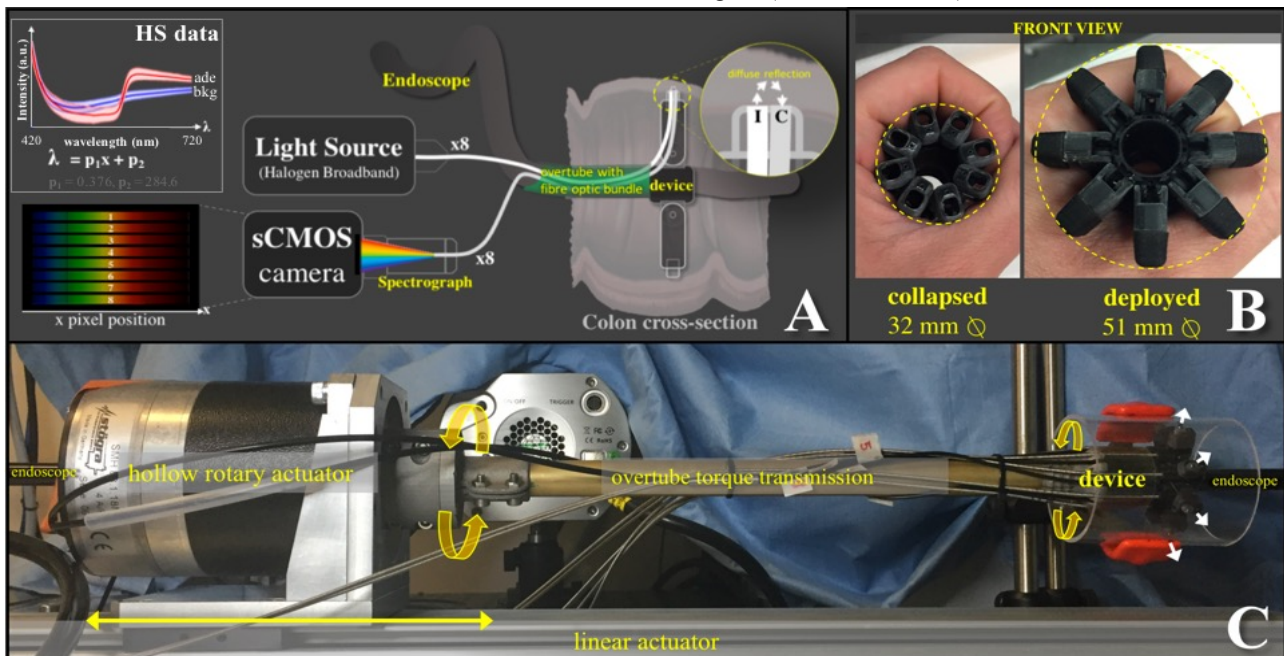


**Fig. 1:** (A) Optical design of an individual DRS sensor: the DRS signal is acquired in each probe by an illumination [I] and a collection [C] fibre (core:cladding=200:20  $\mu\text{m}$ , N.A=0.22). All terminations of the collections fibres are arranged in a 1x8 array (not shown) in front of a spectrograph attached to an sCMOS camera that captures images containing the spectra of each probe. Pre-defined pixel-to-wavelength calibration factors  $p_1$   $p_2$  and white standard references are used to convert spectral images to DRS spectra. Top-left plot: representative 781 DRS spectra (mean  $\pm$ SD) of simulated adenomas (*ade*) vs. 3049 DRS spectra of simulated mucosa (*bkg*). (B) Front-view of the device in a collapsed and deployed configuration. (C) Current fixed scanning mechanism based on a hollow rotary actuator mounted on top of a linear actuator. The device is axially translated as an over-tube add-on to any conventional endoscope.

acquisition, HS data processing and visualisation, are fully integrated into a MATLAB framework. The position of all probes is derived from a single angular and linear position reported by the actuators. Each scanning position is co-registered with its corresponding DRS spectrum. Grayscale images are reconstructed by integrating total intensities from each DRS spectrum. A user interface allows real-time visualisation of acquired raw and processed data as 2D and 3D maps, where the 3D map corresponds to the 2D image texture-mapped to a cylinder, simulating a 3D representation of the colon (Fig. 2, d-e).

## EXPERIMENTAL VALIDATION

This abstract focuses on characterising the optical resolution achievable with the current setup on rigid and deformable targets simulating the colon. For rigid targets, we scanned a plastic tube internally covered with a standard resolution target (1959 USAF). The scanning sequence comprised a 48° partial rotation (step size=1°) while axially advancing the device along the tubular target (step size=0.4 mm). Actuation errors were measured as  $\sqrt{(pos_{ro} - pos_{re})^2}$ , where  $pos_{ro}$  is the rounded pixel coordinate of the reconstructed image, and  $pos_{re}$  is the real position reported by the encoders. As deformable targets, silicone phantoms were manufactured (Ecoflex 00-30). The phantoms included simulated flat lesions (cylindrical features  $\varnothing = 0.5$  to 6.0 mm, height = 0.7 mm) that were pigmented to provide a clear HS signal (*ade*, top-left Fig. 1A) over the simulated mucosa background colour (*bkg*).

## RESULTS

The average angular rotation error of the current device is 0.02° (SD 0.06°). The linear stage positioning error is stated to be at ±0.02 mm. The optical resolution achievable is 0.5 line pairs per mm (Fig. 2a). This optical resolution is consistent with the smallest simulated flat pre-cancerous lesions resolved (0.75 mm), even while the

scanning was performed inside deformable and stretchable phantoms (Fig. 2, b-e).

## DISCUSSION

We report for the first time 2D and 3D reconstruction of endoscopic HS data acquired via robotic scanning of a simulated colon by a radial array of contact single-point DRS probes. Sub-millimetre optical resolution has been demonstrated, which could allow the identification of flat pre-cancerous lesions that are currently missed. The size of the device is compatible with the anatomical dimensions of the colon, but further miniaturisation is desirable. Our work towards the clinical applicability of the device currently concentrates on negotiating the variable diameter, folds, and flexures of the colon. Angular actuation along highly tortuous paths via a torque transmission cable is at the centre of our investigations, as well as the integration of safety features like pressure sensing on the probes. Ultimately, classified HS data could be spatially registered with the video stream of any conventional endoscope. This device will pave the way towards the next generation of augmented reality endoscopy while increasing its sensitivity and specificity.

This work is supported by the Institutional Strategic Support Fund: Networks of Excellence Scheme 2015 (GM), UK ERC award 242991 (DSE) and *Becas Chile* scholarship from the Chilean Government (FBA).

## REFERENCES

- [1] Pawa, N., T. Arulampalam, and J.D. Norton, Screening for colorectal cancer: established and emerging modalities. *Nat Rev Gastroenterol Hepatol*, 2011. 8(12): p. 711-22.
- [2] van Rijn, J.C., et al., Polyp miss rate determined by tandem colonoscopy: a systematic review. *Am J Gastroenterol*, 2006. 101(2): p. 343-50.
- [3] Avila-Rencoret, F., et al, Towards a robotic-assisted cartography of the colon: a proof of concept, in *IEEE ICRA*, Seattle, WA, 2015, pp. 1757-1763.

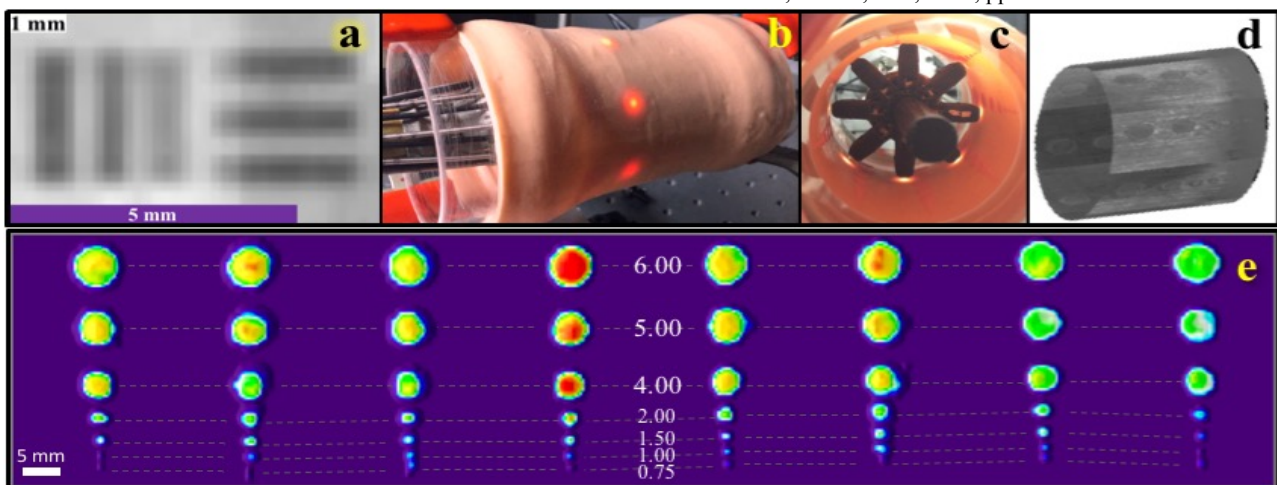


**Fig. 2: In vitro optical resolution validation experiment.** (a) cropped sub-section of a scanned paper 1951 USAF target showing a maximal optical resolution of 0.5 line pairs per mm. (b) External and (c) proximal view of a scanning inside a 5 cm diameter silicone phantom containing patterns of simulated flat pre-cancerous lesions of different diameters. (d) Resulting reconstructed 3D grayscale image (texture mapped from 2D), and (e) 2D image "hotspot" map based on grayscale pixel intensities. It can be seen that the smallest simulated flat pre-cancerous lesions resolved by the device are 0.75 mm in diameter